# Angular analysis and CP violation studies in $B$ decays at CMS

**Kai-Feng Chen**

Department of Physics, National Taiwan University, Taipei, Taiwan

E-mail: Kai-Feng.Chen@cern.ch

**Abstract.** Angular distributions of the decay $B^0 \to K^{*0}\mu^+\mu^-$ are a clean probe of physics beyond the standard model. In particular the forward-backward asymmetry and other variables which can be determined as a function of $q^2$, provide fruitful information from a single decay channel. An angular and proper decay time analysis is applied to the $B_s \to J/\psi\phi$ decays. The $B_s$ signal candidates are reconstructed and used to extract the mixing phase $\phi_s$. The theoretical prediction of the $\phi_s$ angle is particularly robust, thus any deviation from the prediction can be a smoking gun signal of new physics.

## 1. Introduction

The flavor-changing neutral-current decays such as $B^0 \to K^{*0}\mu^+\mu^-$ are of particular interest for new physics searches, since new physics phenomena beyond the standard model can be observed indirectly through their influence in the loop diagram. The decay $B^0 \to K^{*0}\mu^+\mu^-$ can provide many observables, such as the branching fraction, forward-backward asymmetry of the muons ($A_{FB}$), as well as the longitudinal polarization fraction of the $K^{*0}$ ($F_L$), and in particular these observables can be measured as a function of $q^2 = M^2(\mu^+\mu^-)$. Theoretical calculations for these observables are relatively robust, hence any deviation between experimental measurements and the predictions can be interpreted as a hint of the new phenomena (See Ref. [1, 2, 3, 4, 5] for example).

The weak phase $\phi_s$ arises from the interference between direct $B_s$ meson decays into a CP eigenstate $B_s \to J/\psi\phi$ and decays through mixing to the exactly same state. The weak phase $\phi_s$ is related to the CKM matrix elements, where $\phi_s \approx -2\beta_s$, $\beta_s = \arg(-V_{ts}V_{tb}^*/V_{cs}V_{cb}^*)$. Within the standard model, the $\phi_s$ is predicted to be a small value of $-0.0363^{+0.0016}_{-0.0015}$ rad [6]. Since the prediction is rather precise, any deviation of the measured value would be as a possible hint of new physics in the $B_s$ mixing. In particular, many new physics scenarios may enhance the value of $\phi_s$ [7, 8].

The analyses for $B^0 \to K^{*0}\mu^+\mu^-$ and for $B_s \to J/\psi\phi$ are using the data collected by the CMS detector. The CMS detector is a general-purpose detector. A detailed description can be found in Ref. [9]. The central feature of the detector is a superconducting solenoid that provides an axial magnetic field of 3.8 T. Charged particle trajectories are measured within the field volume by pixel and silicon strip tracker. The calorimeter enclosing the tracker includes a lead tungstate crystal electromagnetic calorimeters (ECAL), which is composed of a barrel part and two endcaps, a lead and silicon preshower detector in front of the ECAL endcaps, and a brass/scintillator hadron calorimeter (HCAL) that together provide an energy measurement

for electrons, photons, and hadronic jets. Muons are identified and measured in gas-ionization detectors embedded in the steel return yoke outside the solenoid. The detector is nearly hermetic, allowing accurate energy balance measurements in the plane transverse to the beam direction. The direction of particles measured inside the CMS detector is described using the azimuthal angle ($\phi$) and the pseudorapidity ($\eta$), which is defined as $\eta \equiv -\ln[\tan\theta/2]$, where $\theta$ is the polar angle relative to the counterclockwise proton beam direction, as measured from the nominal interaction vertex.

## 2. Angular analysis of $B^0 \to K^{*0}\mu^+\mu^-$

In this section, the measurements of $A_{FB}$, $F_L$, and the differential branching fraction $d\mathcal{B}/dq^2$ from $B^0 \to K^{*0}\mu^+\mu^-$ decays, using data collected from pp collisions at $\sqrt{s} = 7\,\text{TeV}$ and corresponding to an integrated luminosity of $5\,\text{fb}^{-1}$, are presented. The details of the analysis can be found in Ref. [10].

The signal $B^0 \to K^{*0}\mu^+\mu^-$ decays are recorded with a trigger, which requires two identified muons of opposite charge to form a vertex that is displaced from the beamspot. The trigger configurations were updated during the data taking period with tightening requirements to preserve an acceptable trigger rate. The signal decay mode used in this analysis require two reconstructed muon candidates and two charged hadrons. The muon candidates are required to match the triggered muon in the event and to pass several quality requirements. A muon track must be matched with at least one muon segment, $\chi^2$ per degrees of freedom of track-fit must be less than 1.8, and there must be at least 11 (2) hits in the tracker (pixel detector).

The charged hadron tracks are required to fail the muon selection criteria. The the invariant mass of the two charged hadrons, with either $K^+\pi^-$ or $K^-\pi^+$ hypothesis, must be within a $\pm 80$ MeV mass window around the nominal $K^{*0}$ mass. If the invariant mass with a hypothesis of two charged kaons is below 1.035 GeV, the pair of hadron tracks is rejected for possible $\phi$ meson contributions. The B meson candidates are obtained by requiring the four charged tracks to a common vertex with a constrained fit. The invariant mass of the $B^0$ candidate must be within $\pm 280$ MeV from the world-average mass of $B^0$ meson. The candidate is identified as a $B^0$ or $\overline{B}^0$ if the $K^+\pi^-$ or $K^-\pi^+$ invariant mass is closer to the nominal $K^{*0}$ mass, respectively. In cases where both K-$\pi$ hypotheses are within $\pm 50$ MeV from the $K^{*0}$ mass, the event is rejected from the analysis. With the full selection criteria, there are 8% of the candidates with incorrect b-flavor assignment.

Figure 1 shows the angular observables which define the decay: $\theta_K$ is the helicity angle of the $K^{*0}$ candidate, $\theta_l$ is the helicity angle for the dimuon system, and $\phi$ is the angle between the $K^{*0}$ and dimuon planes. Extraction of the physics parameters, including $A_{FB}$ and $F_L$, do not require the angle $\phi$ and therefore it is integrated out to reduce the complexity. The angular distribution of $B^0 \to K^{*0}\mu^+\mu^-$ can be expressed as:

$$\begin{aligned}\frac{1}{\Gamma}\frac{d^3\Gamma}{d\cos\theta_K d\cos\theta_L dq^2} &= \tfrac{9}{16}\Big\{ \Big[\tfrac{2}{3}F_S + \tfrac{4}{3}A_S\cos\theta_K\Big](1-\cos^2\theta_L) \\ &\quad +(1-F_S)\Big[2F_L\cos^2\theta_K(1-cos^2\theta_L) \\ &\quad +\tfrac{1}{2}(1-F_L)(1-\cos^2\theta_K)(1+\cos^2\theta_L) \\ &\quad +\tfrac{4}{3}A_{FB}(1-\cos^2\theta_K)\cos\theta_L\Big]\Big\}\,,\end{aligned}$$

where the $F_S$ and $A_S$ are the S-wave faction and the interference amplitude between the S- and P-wave decays, respectively. The result of the analysis is extracted from unbinned extended maximum-likelihood fits in bins of $q^2$ to the invariant mass of the $B^0$ meson candidate, and the two angles $\theta_K$ and $\theta_l$, using the angular distribution model introduced above. After excluding

the $q^2$ regions corresponding to $J/\psi$ and $\psi'$ resonances, there are total $415 \pm 30$ signal events distributed in 6 $q^2$ bins.

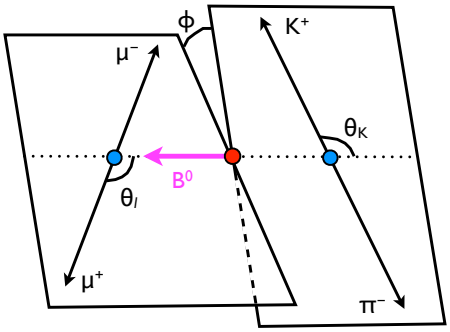


**Figure 1.** The definition of the angular observables for the $B^0 \to K^{*0}\mu^+\mu^-$ decay.

The measured values of $F_L$, $A_{FB}$, and differential branching fractions in bins of $q^2$ are summarized in Fig. 2, along with the standard model predictions. The results are found to be consistent with the predictions, as well as with measurements from other experiments. The CMS results for this decay channel are competitive with other experiments, in particular for the higher $q^2$ bins. The analysis with full 2012 data sets will provide further information in this decay. These results can be used to constrain the new physics beyond the standard model in the near future.

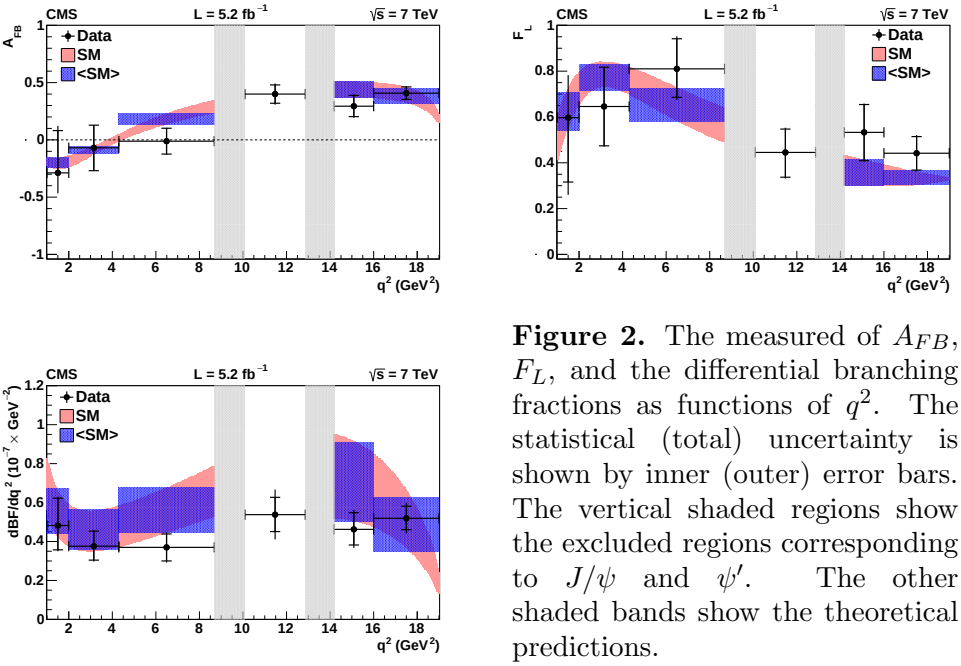


**Figure 2.** The measured of $A_{FB}$, $F_L$, and the differential branching fractions as functions of $q^2$. The statistical (total) uncertainty is shown by inner (outer) error bars. The vertical shaded regions show the excluded regions corresponding to $J/\psi$ and $\psi'$. The other shaded bands show the theoretical predictions.

### 3. Measurement of the CP-violating weak phase $\phi_s$ in $B_s \to J/\psi\phi$ decays

The weak phase $\phi_s$ is measured with $B_s \to J/\psi\phi$ decays, which does not have a definite CP state and an angular analysis is required to disentangle the CP-odd and CP-even components of the final state. A time-dependent angular analysis is introduced by measuring the decay angles of the final state particles and the proper decay length of the $B_s$. In this analysis a dataset

corresponding to an integrated luminosity of $20\,\text{fb}^{-1}$ collected from pp collisions at $\sqrt{s} = 8\,\text{TeV}$ is used. The details of the analysis can be found in Ref. [11].

The $B_s \to J/\psi\phi$ signal events are triggered with a $J/\psi$ candidate displaced from the primary vertex. In the offline section, the muons are required to have a minimum $p_\text{T}$ of 4 GeV. Two oppositely charged muons are paired and form a common decay vertex. Dimuon pairs are selected if the invariant mass is within $\pm 150$ MeV of the average $J/\psi$ mass. The $\phi \to K^+K^-$ candidates are reconstructed using pairs of oppositely charged tracks with nominal kaon mass assumed. The invariant mass of the $K^+K^-$ pair is required to be within a $\pm 10$ MeV mass window around the nominal $\phi$ mass.

The $B_s$ candidates are reconstructed from the $J/\psi$ candidate and $\phi$ meson candidates. A common vertex position and its associated uncertainty are determined from a fit to all four final state charged tracks, constraining the dimuon invariant mass to the $J/\psi$ mass. For events with multiple $B_s$ candidates, the candidate with the best vertex fit quality is selected. The proper decay length, $ct$, is calculated based on the vertex position of $B_s$ candidate. The proper decay length is required to be larger than 200 $\mu$m in order to avoid a bias due to the turn-on curve from the trigger.

In this analysis, the angular distribution is defined in the transversity basis [12]. The definitions of the three angles $\Theta = (\theta_T, \psi_T, \phi_T)$ are illustrated in Fig. 3. The angle $\theta_T$ ($\phi_T$) is the polar (azimuthal) angle defined of the $\mu^+$ in the $J/\psi$ rest frame, while the angle $\psi_T$ is the helicity angle of $\phi$ meson defined by the direction of $K^+$. The differential decay rate for $B_s \to J/\psi\phi$ can be expressed as:

$$\frac{d^4\Gamma[B_s(t)]}{d\Theta dt} = \sum_{i=1}^{10} \mathcal{O}_i(\alpha, t) \cdot g_i(\Theta) \ ,$$

where $\mathcal{O}_i$ are the time-dependent functions and $g_i$ are the angular-dependent functions. The $\alpha$ are the physics parameters of interests; the $\Theta$ and $t$ represent the measured angles and proper decay time of the $B_s$ decay. The function $\mathcal{O}_i$ can be expanded as:

$$\mathcal{O}_i(\alpha, t) \propto e^{-\Gamma_s t}\left[a_i \cosh\left(\tfrac{1}{2}\Delta\Gamma_s t\right) + b_i \sinh\left(\tfrac{1}{2}\Delta\Gamma_s t\right) + c_i \cos\left(\Delta m_s t\right) + d_i \sin\left(\Delta m_s t\right)\right] \ ,$$

where the parameters $b_i$ and $d_i$ contain the contribution from the weak phase $\phi_s$. The details of the description of the time-dependent decay rate can be found in Ref. [13].

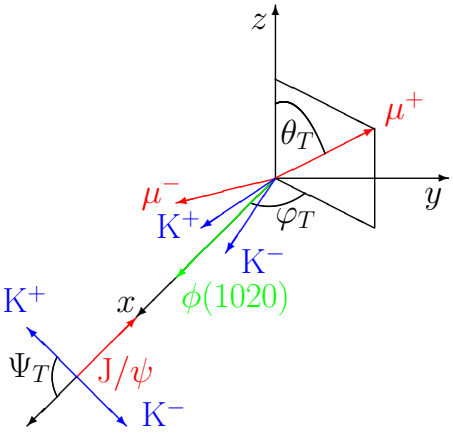


**Figure 3.** Definition of the three angular observables, $\theta_T$, $\psi_T$, and $\phi_T$ for the $B_s \to J/\psi\phi$ decays.

Another important ingredient of this analysis is the capability of flavor tagging. If the other b-hadron opposite to the signal $B_s$ candidate decays in one of the semileptonic channels, the charge of the opposite-side muon or electron is used to derive the flavor of the signal $B_s$ meson

at its production time. In practise the lepton with the highest $p_{\mathrm{T}}$ in the event is used as the tagging lepton. The tag lepton selection is optimized to reach the best tagging power, $P_{\mathrm{tag}} = \epsilon_{\mathrm{tag}}(1-2\omega)^2$, where the $\epsilon_{\mathrm{tag}}$ is the tagging efficiency and $\omega$ is the mis-tag probability. The performance of the tagging is measured from the data with the self-tagging $B^+ \to J/\psi K^+$ decays. The measured average tagging performance with electron and muon taggers combined is $\omega = (32.3 \pm 0.3)\%$, $\epsilon_{\mathrm{tag}} = (7.67 \pm 0.04)\%$, and resulting $P_{\mathrm{tag}} = (0.97 \pm 0.03)\%$. The performance evaluated for simulated $B^+$ and $B_s$ events are found to be consistent with each other.

An unbinned maximum likelihood fit is introduced to extract the physics parameters: the weak phase $\phi_s$, the lifetime difference $\Delta\Gamma_s$, the mean lifetime of $B_s$ meson, the decay amplitudes and the corresponding strong phases. The fit is performed by including information on the candidate $B_s$ invariant mass, proper decay length, and the three decay angles. The per-event proper decay length uncertainty is included in the proper decay time resolution model. The fit sample contains around 49,000 signal events and 21,000 background events. The projections of the three decay angles are shown in Fig. 4, and the resulting physics parameters are summarized in Tab. 1. The value of weak phase $\phi_s$ and the lifetime difference $\Delta\Gamma_s$ are in good agreement with the previous measurements and with the standard model predictions. Our measurements are the second best measurements to date and will improve the world averages. The uncertainties of the measurements are still dominated by statistical uncertainties and can be reduced further with upcoming new data from LHC run II.

**Table 1.** The measured physics parameters of interests from the unbinned maximum likelihood fit to the $B_s \to J/\psi\phi$ candidates.

| Parameter | Result |
|---|---|
| $\lvert A_0\rvert^2$ | $0.511 \pm 0.006 \pm 0.012$ |
| $\lvert A_S\rvert^2$ | $0.015 \pm 0.016 \pm 0.022$ |
| $\lvert A_\perp\rvert^2$ | $0.242 \pm 0.008 \pm 0.012$ |
| $\delta_\parallel$ | $3.48 \pm 0.09 \pm 0.68$ rad |
| $\delta_{S\perp}$ | $0.34 \pm 0.24 \pm 1.12$ rad |
| $\delta_\perp$ | $2.73 \pm 0.36 \pm 0.66$ rad |
| $c\tau$ | $447.3 \pm 3.0 \pm 3.5$ $\mu$m |
| $\Delta\Gamma_s$ | $0.096 \pm 0.014 \pm 0.007$ ps$^{-1}$ |
| $\phi_s$ | $-0.03 \pm 0.11 \pm 0.03$ rad |

## References


[1] Q. S. Yan, C. S. Huang, W. Liao and S. H. Zhu, "Exclusive semileptonic rare decays $B \to (K, K^{*)}\ell^+\ell^-$ in supersymmetric theories," Phys. Rev. D **62**, 094023 (2000) [hep-ph/0004262].

[2] W. Altmannshofer, P. Ball, A. Bharucha, A. J. Buras, D. M. Straub and M. Wick, "Symmetries and Asymmetries of $B \to K^*\mu^+\mu^-$ Decays in the Standard Model and Beyond," JHEP **0901**, 019 (2009) [arXiv:0811.1214 [hep-ph]].

[3] A. Ali, P. Ball, L. T. Handoko and G. Hiller, "A Comparative study of the decays $B \to (K, K^{*)}\ell^+\ell^-$ in standard model and supersymmetric theories," Phys. Rev. D **61**, 074024 (2000) [hep-ph/9910221].

[4] G. Buchalla, G. Hiller and G. Isidori, "Phenomenology of nonstandard $Z$ couplings in exclusive semileptonic $b \to s$ transitions," Phys. Rev. D **63**, 014015 (2000) [hep-ph/0006136].

[5] T. Feldmann and J. Matias, "Forward backward and isospin asymmetry for $B \to K^*\ell^+\ell^-$ decay in the standard model and in supersymmetry," JHEP **0301**, 074 (2003) [hep-ph/0212158].

[6] J. Charles, O. Deschamps, S. Descotes-Genon, R. Itoh, H. Lacker, A. Menzel, S. Monteil and V. Niess *et al.*, "Predictions of selected flavour observables within the Standard Model," Phys. Rev. D **84**, 033005 (2011) [arXiv:1106.4041 [hep-ph]].

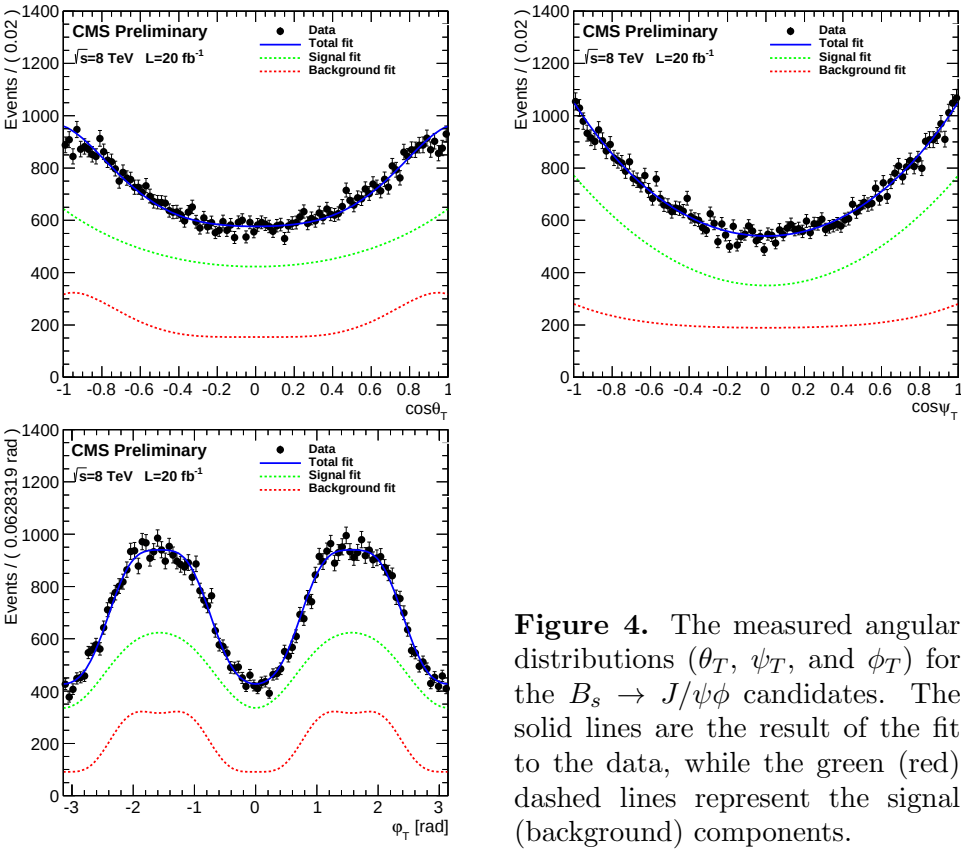


**Figure 4.** The measured angular distributions ($\theta_T$, $\psi_T$, and $\phi_T$) for the $B_s \to J/\psi\phi$ candidates. The solid lines are the result of the fit to the data, while the green (red) dashed lines represent the signal (background) components.


[7] A. J. Buras, "Flavour Theory: 2009," PoS EPS **-HEP2009**, 024 (2009) [arXiv:0910.1032 [hep-ph]].

[8] C. W. Chiang, A. Datta, M. Duraisamy, D. London, M. Nagashima and A. Szynkman, "New Physics in $B_s^0 \to J/\psi\phi$: A General Analysis," JHEP **1004**, 031 (2010) [arXiv:0910.2929 [hep-ph]].

[9] S. Chatrchyan *et al.* [CMS Collaboration], "The CMS experiment at the CERN LHC," JINST **3**, S08004 (2008).

[10] The CMS Collaboration, "Angular analysis and branching fraction measurement of the decay $B^0 \to K^{*0}\mu^+\mu^-$," Phys. Lett. B **727**, 77 (2013) [arXiv:1308.3409 [hep-ex]].

[11] The CMS Collaboration, "Measurement of the CP-violating weak phase $\phi_s$ and the decay width difference $\Delta\Gamma_s$ using the $B_s \to J/\psi\phi$ decay channel," CMS PAS BPH-13-012 (2014).

[12] A. S. Dighe, I. Dunietz and R. Fleischer, "Extracting CKM phases and $B_s - \bar{B}_s$ mixing parameters from angular distributions of nonleptonic $B$ decays," Eur. Phys. J. C **6**, 647 (1999) [hep-ph/9804253].

[13] A. S. Dighe, I. Dunietz, H. J. Lipkin and J. L. Rosner, "Angular distributions and lifetime differences in $B_s \to J/\psi\phi$ decays," Phys. Lett. B **369**, 144 (1996) [hep-ph/9511363].